Heat Transfer

WILEY

HEAT TRANSFER

ORIGINAL ARTICLE OPEN ACCESS

Experimental Investigation of Parameters Influencing Test Box and Material Behavior in Daytime Radiative Cooling Measurements

M. Reda Haddouche | Ingrid Martorell | Cristian Solé | Albert Castell | Marc Medrano

Sustainable Energy, Machinery and Buildings (SEMB) Research Group, INSPIRES Research Centre, Universitat de Lleida, Lleida, Spain

Correspondence: Marc Medrano (marc.medrano@udl.cat)

Received: 25 February 2025 | **Revised:** 3 April 2025 | **Accepted:** 6 April 2025

Funding: This publication is part of the grant PID2021-126643OB-I00, funded by MCIN/AEI/10.13039/501100011033/and by "ERDF A way of making Europe." This publication is part of the grant TED2021-131446B-I00, funded by MCIN/AEI/10.13039/501100011033/and by the "European Union NextGenerationEU/PRTR." This publication is also part of the grant PDC2022-133215-I00, funded by MCIN/AEI/10.13039/501100011033/and by the "European Union NextGenerationEU/PRTR."

Keywords: daytime radiative cooling | heat transfer | infrared emissive material | infrared radiation | test box

ABSTRACT

Nowadays, renewable energies are employed to reduce fossil fuel consumption in buildings and industrial applications. Radiative cooling (RC) technology uses the Earth's natural heat radiation to cool surfaces without any electricity supply by emitting thermal radiation to outer space through the transparent atmospheric window. RC technology can produce a cooling effect both during the night and during the day. However, daytime RC is a challenge, and special materials are to be used. Materials highly reflective in the solar spectrum (0.3–2.5 μm), and highly emissive in the atmospheric IR transparency window (8–13 μm) are required for daytime RC technology. This study explores the influence of several parameters in the design of the daytime RC materials testing set-up (test box), aiming ultimately at an effective measurement and evaluation of RC materials during daylight hours using a test box. The approach utilizes a test box setup to assess the materials' ability to emit thermal radiation while under the influence of direct sunlight. By employing precise measurement techniques within this controlled environment, this study contributes to the identification of key parameters affecting daytime RC materials measurements. The outcomes of this investigation contribute to the ongoing efforts in the field of daytime RC, offering practical guidance for researchers, engineers, and designers involved in developing a test box for daytime RC materials testing.

1 | Introduction

Radiative cooling (RC) technology utilizes the Earth's natural heat radiation to freely cool surfaces, devoid of any reliance on electricity, by emitting thermal radiation to outer space through the atmospheric transparent window. RC technology has some advantages, such as simple structure, simple manufacturing process, low cost, and wide applicability [1]. This technology consists of obtaining cooling power without external energy input [2]. To effectively implement RC, materials with high reflectivity in the solar spectrum (0.3–2.5 μm) and high emissivity within the atmospheric IR transparency window (8–13 μm) are essential [3–7]. This technology enables cooling both during nocturnal hours and daytime periods. Nonetheless, achieving effective daytime radiative cooling (DRC) poses a significant challenge since special materials are needed. Constructing a test box that allows the evaluation of DRC materials involves several key strategies to ensure accurate and controlled experimentation. Typically, the appropriate materials for the test box construction include thermal insulating foams, reflective surfaces, and transparent materials in the infrared range. Many researchers are focused on the design of a test box for RC

using different measurement techniques and strategies to show the reliability of the DRC materials [8].

Raman et al. [9] pioneered the development of DRC materials; thus, they also constructed an apparatus to test their innovative DRC material. They used a tilted apparatus of 30° for temperature measurement of the daytime RC under the sunlight that minimizes the convective and conductive heat. In their experiment, a 20 cm silicon wafer that serves as the RC surface is set on a polystyrene pedestal that is held up by a transparent acrylic box, and above the sample, a clear 12.5 μm polyethylene sheet serves as an infrared-transparent windshield. They reported that their experimental restriction limits the amount of sky access available for thermal radiation. Three years later, Kou et al. [10] stated that extra care must be taken in the measuring setup to minimize parasitic conduction and convection from the environment to experimentally achieve cooling below ambient. In their investigation, the box is set up on an aerogel blanket with low heat conductivity that is fastened to the inside of a Petri dish. A polyethylene film covers the top of the Petri dish, serving as a convection shield. Tso et al. [11] suggested using vacuum technology in a test box to eliminate heat loss by conduction and convection to maximize the thermal performance of the sample as a passive radiative cooler. Their proposed design consists of a passive RC sample located inside the vacuum chamber (Test box), and they use seven potassium chloride IR-pass windows of 10 cm diameter and 23 mm thick as the cover of the vacuum chamber. The test box is covered by aluminum on its inner and outer walls. Their results showed that this type of test box provided sub-ambient cooling during the night; meanwhile, during the day, the temperature was above the ambient temperature.

Ao et al. [12] investigated experimentally the cooling performance of DRC samples. The equipment used in their investigation is a test box of dimensions 40 × 40 × 10 cm. The thickness of the bottom insulating layer is 8 cm. A sample of dimensions 15 × 15 cm is used as a RC surface and positioned in the horizontal center of the box. Low-density polyethylene film of thickness 20 μm is used as a windshield to prevent convection since it has high transmissivity at nearly all wavelengths. The box is covered with aluminum foil, except for the sample of RC material. Li et al. [13] investigated the optical properties and structure of aluminum phosphate for daytime passive RC applications. The test box made from polystyrene foam, with low heat conductivity, of thickness 3 cm has a size of 15 × 20 × 15 cm. Moreover, aluminum foil is wrapped around polystyrene to minimize heat intake and remove most of the impact from thermal conduction.

Liu et al. [14] designed a parallelepiped test box for testing daytime RC materials. The test box was made of polystyrene foam and was covered by aluminum foil to reflect the solar radiation. They used a sample of 10 × 10 cm as RC material. A wind cover made of 10 μm polyethylene film was used to decrease the effect of non-radiative heat exchange from the top side of the box. Additionally, they suggested using a temperature-controlled electric heater to elevate the radiative cooler's temperature to test the sample's cooling power in an environment with high humidity. Han et al. [15] designed a wooden test box for testing RC materials. In their study, they suggested minimizing heat conduction; for this, the sample should be supported by 60-mm thick polystyrene foam with the same cross-sectional area. The polystyrene foam was positioned in the center of the transparent acrylic chamber, which was held up by a 21.8 cm height wooden frame and covered with aluminum foil to avoid heating from incoming solar radiation and to minimize convection over the sample. They suggested using a 12 μm low-density polyethylene film on the upper surface of the hardwood frame. Liu et al. [16] performed tests to give insight into the importance of adding or not a wind cover. They presented an experimental device constructed with a 30 × 30 × 4 cm square box of high transparent polymethyl methacrylate to decrease sun absorption. A 10 μm polyethylene film was used as wind cover at the top of the box to guarantee strong solar and mid-infrared light transmission while minimizing non-radiative heat exchange between the radiative cooler and its surroundings. To lessen heat transmission between the radiative cooler and the device, a 2 cm thick piece of polystyrene foam was affixed to the bottom of the square box, which housed the radiative cooler. Later, Wong et al. [17] reported materials preparation procedures as well as the fabrication of the outdoor setup field on the rooftop of the campus of The Hong Kong University of Science and Technology, for surface temperature measurement for both daytime and nighttime RC. In their study, the RC material was set up on an acrylic ring support, put inside a glass Petri dish, and covered with a polyethylene film. The supporting structure that held the assembly was resting on an aerogel blanket.

Some researchers have tested hybrid RC materials. For example, Zhai et al. [18] proposed a structure of the randomized glass-polymer hybrid metamaterial as DRC material, using micrometer-sized SiO_2 spheres that are dispersed randomly in the polymethyl pentene matrix material. The polymer metamaterial is tested by placing it into a foam container to reduce the parasitic heat transfer. They reported an average daytime RC power of 110 $W \cdot m^{-2}$, and an average cooling power of 93 $W \cdot m^{-2}$ when the solar irradiation is 900 $W \cdot m^{-2}$. Zhang et al. [19] tested the cooling performance of a hybrid RC ZrO_2/PDMS in a 30 × 30 × 20 cm polystyrene test box with the lateral walls of the polystyrene box covered with aluminum foil to reflect the solar radiation. A polyethylene film was used above the test box as a windshield to reduce the influence of convection. Xiang et al. [20] designed an outdoor apparatus to test a hybrid material for outdoor passive RC based on a 3D porous cellulose acetate film. The test boxes consisted of a 30 × 30 × 15 cm polystyrene foam block with a 15 cm diameter × 3 cm cylindrical grove. The foam block was covered by aluminum foil, and no windshield was used. Outdoors tests showed cooling temperatures of 8.6°C and 6.2°C for nighttime and daytime, respectively.

Park et al. [21] used a 30 × 40 × 30 cm polystyrene foam box covered with a silver reflective film. A polyethylene windshield was placed to minimize convective heat transfer, and tests were performed to determine the cooling performance of a DRC coating using raspberry-like hollow SiO_2 spheres. Recently, Liu et al. [22] presented an experimental study of thin paint for durable and scalable RC. They conducted an outdoor experiment to investigate the RC and heat dissipation properties of the designed thin durable paint using a test box. The thin paint was

placed on a foam box, with a heater fixed beneath for heat dissipation analysis. The proposed paint achieved a high solar reflectance of 0.963 and thermal emittance of 0.927 at 150 μm thickness. They reported that a 2.3°C lower temperature is reached in comparison to standard PDRC coatings, and an enhanced heat dissipation resulted from using this thin paint. Lee et al. [23] built a test box to assess the performance of a hybrid RC material (polydimethylsiloxane as a binder and mixed with hollow silica spheres). A $30 \times 40 \times 30$ cm polystyrene block covered with a reflective film and shielded with a 30 μm LDPE windshield was used. Outdoor experiments were performed in South Korea in July 2023, and temperatures of 7.6°C and 4°C below the ambient temperature were recorded. Yu et al. [24] used a styrene foam covered with aluminum Mylar tape and covered the top side of the styrene box with LDPE film. Experiments were carried out in South Korea in November 2021 to test the potential of integrating hollow Yttrium-Oxide spheres within a polydimethylsiloxane matrix; 9.8°C temperatures below ambient temperature during daytime were registered.

All the previous studies show the difficulties of constructing a test box for testing RC materials. In the literature, several researchers gave some instructions on how to build the test box for evaluating RC materials, and different shapes and geometries of test boxes were presented. The most common typology of test boxes found in the literature is the one consisting of a parallelepiped casing with insulation in the bottom and the RC material placed on top of it. However, different researchers develop their own test boxes, and inconsistencies are observed in the literature regarding some critical parameters. Thus, further research is warranted to identify critical parameters that affect the measurement. The main objective of this study is to investigate the parameters that have an impact on the test box behavior and, consequently, the sample's performance during the measurement of the daytime RC materials. In this study, the impact of various parameters that can affect the thermal behavior of the test box and the temperature of the RC materials are investigated under the real climatic conditions of a temperate semi-arid climate (in Lleida, Spain). The coating material for the lateral walls of the test box and the use of a windshield cover are two of the main parameters that have variations in the test boxes found in the literature. Moreover, the influence of solar protection on the enclosed air temperature sensor is critical for the correct characterization of RC. Finally, the effect of the substrate material on the RC material may also play a role in its behavior. Thus, these four parameters will be studied and analyzed in this study. The results of this study add to the current body of knowledge on the subject of daytime RC by providing helpful guidance to scientists, engineers, and designers who are working on developing a test box for materials testing related to daytime RC.

2 | Materials and Methods

RC is a renewable cooling technology that utilizes specially engineered surfaces and materials to emit infrared (IR) radiation in the atmospheric window (8–13 μm), enabling objects to cool down by radiating heat into the cold space.

The energy balance that occurs within the RC surface is shown in Figure 1.

And the net cooling power is estimated as the below equation.

$$P_{\text{cooling}} = P_{\text{rad}} - P_{\text{sun}} - P_{\text{atm}} - P_{\text{conv+cond}}. \quad (1)$$

In this equation,

P_{rad}: is the RC power,

P_{sun}: is the incoming solar irradiation,

P_{atm}: is the atmospheric radiation,

$P_{\text{conv+cond}}$: is the convective and conductive heat.

Material selection is essential when constructing RC test boxes. Thermal insulating foams are used to minimize conductive heat transfer, reducing thermal exchange between the sample and the environment. Reflective surfaces are commonly employed in test boxes for daytime RC (DRC) to reflect solar radiation and prevent overheating. Additionally, infrared-transparent materials are typically used as windshield covers to allow IR radiation to pass through while minimizing convective heat gains.

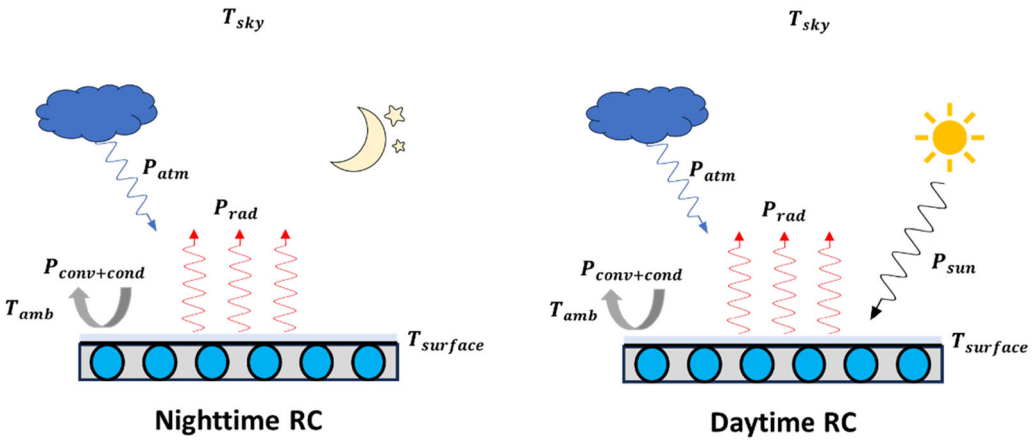

FIGURE 1 | Radiative cooling energy balance. [Color figure can be viewed at wileyonlinelibrary.com]

3 | Description of the Test Box

The test box considered in this study is a parallelepiped wooden box used as a solid structure, with external dimensions of $32 \times 32 \times 16$ cm and a thickness of 2 cm (Figure 2).

The wooden box is used as a solid structure, and it is filled with polystyrene foam 12 cm thick and a thermal conductivity of $k = 0.024\ \mathrm{W \cdot m^{-1} \cdot K^{-1}}$ to insulate the bottom surface of the sample. The lateral surfaces of the box should be covered with a highly reflective material layer in the solar spectrum to reflect the maximum amount of solar radiation and prevent overheating. The sample is put on the middle of the polystyrene upper surface. The remaining surfaces of the polystyrene foam facing the sky are also covered by the same highly reflective layer with the objective of protecting the test box from heat gain. The background surface in the figure refers to the solar reflective material facing the sky, on the upper surface of the polystyrene foam. Finally, the test box should be covered by an infrared transparent windshield to prevent the condensation of the moisture air on the sample and to reduce the heat transfer between the ambient air and the sample. The windshield used in this test box is a 60 μm thick low-density polyethylene film. The sample (21 × 16 cm) is painted with CHILLSKYN coating [25–27] over a thin substrate, which in our case is 0.5 mm thick copper. The Infrared emissivity of the CHILLSKYN paint is $\varepsilon_{IR} = 0.97$, and the solar reflectivity is $\rho_{\mathrm{solar}} = 0.96$.

To well describe the heat transfer phenomena inside and outside the test box, a detailed schematic diagram of the heat transfer that occurs within the test box is shown in Figure 3.

4 | Measurement Procedure

To show the behavior of the RC materials under real climatic conditions and to monitor the parameters surrounding the test setup, such as the ambient temperature and solar radiation intensity, a meteorological station that consists of a pyranometer (Figure 4a) (SMP6, with an accuracy of $\pm 8\ \mathrm{W \cdot m^{-2}}$),

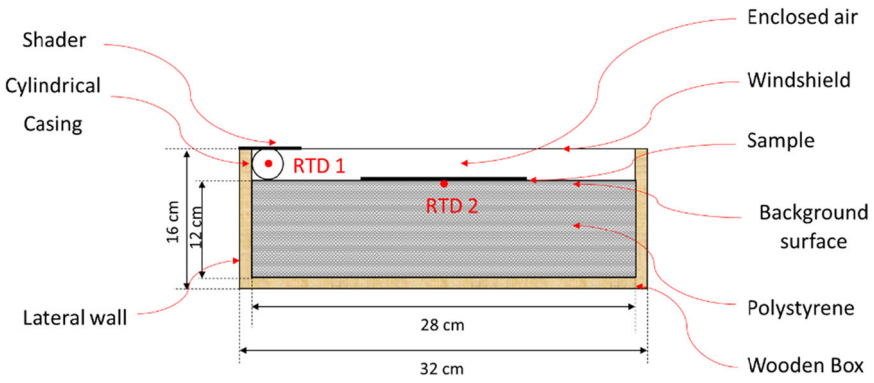

FIGURE 2 | Schematic diagram of the test box. [Color figure can be viewed at wileyonlinelibrary.com]

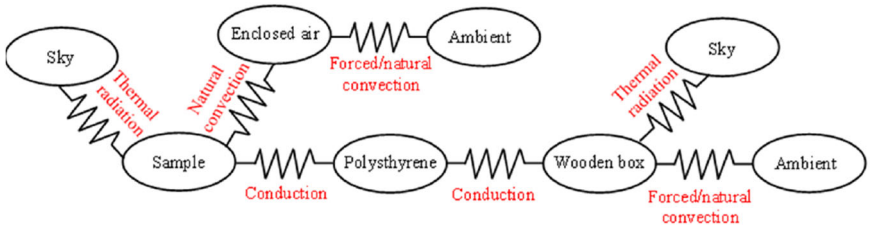

FIGURE 3 | Schematic diagram of the thermal resistance within the test box. [Color figure can be viewed at wileyonlinelibrary.com]

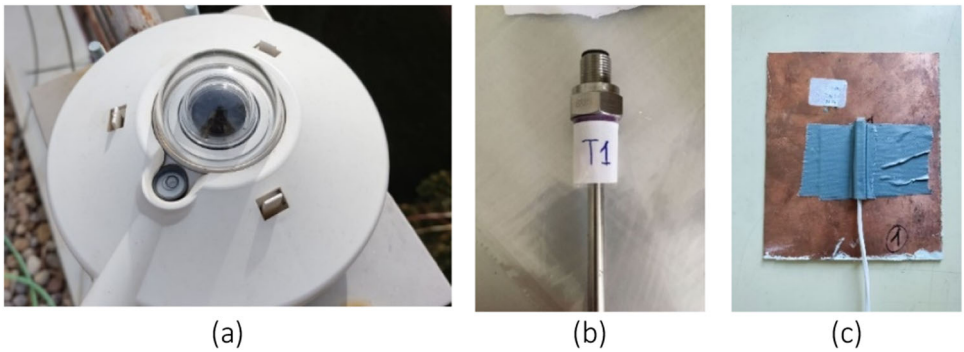

FIGURE 4 | Pyranometer SMP6 (a), enclosed air temperature sensor RTD-PT100 (b), and surface temperature sensor RTD-PT100 (c). [Color figure can be viewed at wileyonlinelibrary.com]

and an ambient temperature sensor (with probe uncertainty of 1/10 DIN and ±0.05 °C unit uncertainty) is used. The ambient temperature is measured using the RTD PT100, as shown in Figure 4b. A Stevenson shield is used to cover the ambient temperature RTD sensor and protect it from direct solar radiation. The Stevenson shield is installed at the same level as the test boxes, about 1 m above the roof ground.

The test box has two calibrated temperature sensors type RTD PT100 (with probe uncertainty of 1/10 DIN and ±0.05°C unit uncertainty); one is used to measure the enclosed air temperature (RTD1) (Figure 4b), and the other one is a contact RTD sensor used to measure the sample temperature (RTD2) (Figure 4c), as shown by the red points in Figure 2.

Finally, an RTD surface temperature sensor is attached at the center of one lateral wall to monitor the surface temperature of the wall of the test box (Figure 5).

5 | Methodology

Daytime RC materials testing involves evaluating materials that can efficiently radiate heat and achieve cooling even in the presence of sunlight. A series of tests before the DRC sample measurements are performed to obtain a reliable test box. A side-by-side methodology is used to determine the influence of each studied parameter. Thus, three identical test boxes have been constructed and are used in the experiments, allowing the change of only one parameter and identifying and quantifying its influence on the temperature measurement of the daytime RC sample. Four main parameters are studied (coating of lateral walls, use of windshield, protection of the enclosed air temperature sensor, and substrate material), as explained in the following paragraphs.

FIGURE 5 | Temperature sensor on the lateral walls of two test boxes. [Color figure can be viewed at wileyonlinelibrary.com]

To reflect the incident solar radiation and prevent the test box from overheating during the daytime, the lateral walls of the test box are covered by reflective surfaces. Two materials are considered: aluminum foils and white paper, both with high solar reflectivity. For this experiment, two test boxes are used; one is covered by white paper on its lateral walls, and the other one is covered by aluminum foil. To analyze the impact of the coating of the lateral wall on the thermal behavior of the test box, the temperature of the lateral wall is monitored and compared.

The impact of the windshield is also investigated. For this experiment, two test boxes with aluminum foil in the lateral walls are used. One of the test boxes is covered at the top by a 0.6 μm thick LDPE film used as a windshield, while the other one is uncovered (Figure 6). To analyze the impact of the windshield on the thermal behavior of the DRC material and the test box, the temperatures of the DRC material and the enclosed air are monitored and compared.

Accuracy in the measurement of the temperature of the enclosed air in the test box is relevant. The impact of protecting the temperature sensor using a cylindrical casing and a shader is also investigated. For that, three different materials (aluminum, white paper, and cardboard) of the same size are tested as shaders. Additionally, the temperature sensor in the enclosed air between the Polystyrene foam and the LDPE film is heated up by the reflection of solar radiation from the background material. Thus, to prevent this bounced solar radiation from the bottom, a cylindrical tube made from cardboard covered with white paper is used as a casing for the enclosed air temperature sensor, as shown in Figure 7. The enclosed air temperature sensor is covered by a cylindrical casing, and the white paper shader is in one test box. The other test box contains an enclosed air temperature sensor without the cylindrical casing and is protected by the white paper shader. To analyze the impact of the protection of the enclosed air temperature

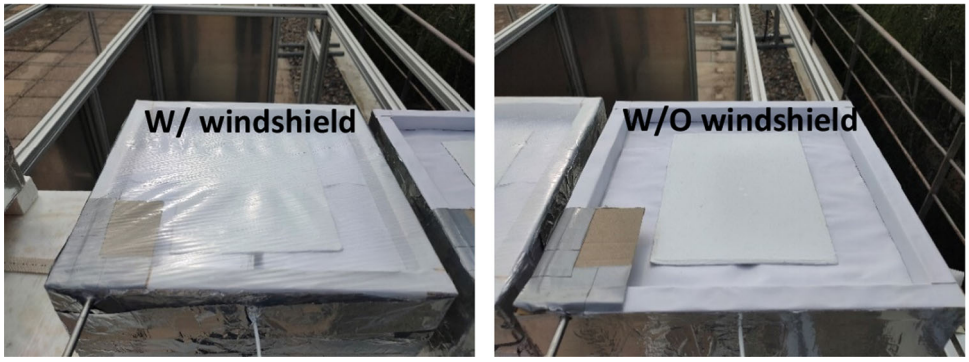

FIGURE 6 | Test boxes with and without a windshield. [Color figure can be viewed at wileyonlinelibrary.com]

sensor on the thermal behavior of the test box, the temperature of the enclosed air is monitored and compared, and thermal imaging is used to visualize temperature differences among shaders.

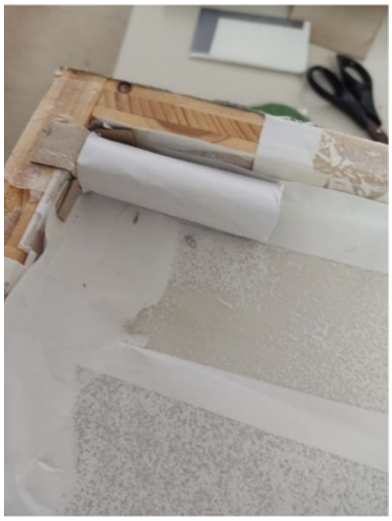

FIGURE 7 | Cylindrical casing for the enclosed air temperature sensor. [Color figure can be viewed at wileyonlinelibrary.com]

FIGURE 8 | Photography of the sample (copper substrates with CHILLSKYN DRC material). [Color figure can be viewed at wileyonlinelibrary.com]

Finally, a case study of daytime RC material behavior is studied. The substrate material studied is copper, which has dimensions 21×16 cm and is 0.5 mm thick. The substrate is painted with CHILLSKYN paint, used as DRC material (Figure 8). To analyze the impact of the substrate material on the thermal behavior of the RC material, the temperature of the RC material sample is monitored. A free-floating test was performed, where the temperature of the sample was left to evolve because of the heat exchange between the sample and the surroundings (mainly by solar and thermal radiation), as shown in Figure 9.

Table 1 summarizes the experiments performed, the boundary conditions for each experiment, and the control variable used to determine the influence of the parameter under study.

6 | Results and Discussion

This section of the paper discusses the test results to show the effects of several parameters that may have an impact on the test box's behavior as well as the samples' temperature. In the last part of this section, the impact of the substrate material of the DRC sample is analyzed.

6.1 | Impact of the Lateral Walls' Coating

In this section, the impact of the coating used on the lateral walls of the test box is examined by considering two materials: white paper and aluminum foil.

The temperature evolution during 18 h of the lateral walls of the two test boxes is shown in Figure 10. The temperature of the two test boxes' lateral walls increases during the day because of the incident solar radiation on the walls. The temperature of the test box lateral wall covered by aluminum foil is lower than the temperature of the test box covered by white paper. This is probably due to the slightly higher solar reflectivity of the aluminum foil (typical values in the range 70%–80%) over that of the white paper (typical values for white paper in the range 60%–80%) [28]. No differences are observed between 1:00 p.m.

FIGURE 9 | Photography of the test facility. [Color figure can be viewed at wileyonlinelibrary.com]

TABLE 1 | Summary of experiments, boundary conditions, and control variables.

Test	No of test boxes/ shaders		Lateral walls	Background	Windshield	DRC material (sample)	Shader	Cylindrical casing	Control variable
Lateral wall coating	2 test boxes	1	White paper	White paper	LDPE 60 μm	Without DRC sample	Cardboard	Without cylindrical casing	Lateral wall temperature
		2	Aluminum foil	White paper	LDPE 60 μm	Without DRC sample	Cardboard	Without cylindrical casing	
Windshield	2 test boxes	1	Aluminum foil	White paper	LDPE 60 μm	Copper (1 mm) + CHILLSKYN	Cardboard	Without cylindrical casing	DRC material temperature and Enclosed air temperature
		2	Aluminum foil	White paper	Without windshield	Copper (1 mm) + CHILLSKYN	Cardboard	Without cylindrical casing	
Enclosed air Temperature—Cylindrical casing	2 test boxes	1	Aluminum foil	White paper	LDPE 60 μm	Cooper (0.5 mm)	White paper	Using cylindrical casing	Enclosed air temperature
		2	Aluminum foil	White paper	LDPE 60 μm	Cooper (0.5 mm)	White paper	Without cylindrical casing	
Substrate material	1 test boxes	1	Aluminum foil	White paper	LDPE 60 μm	Cooper (0.5 mm)	White paper	Using cylindrical casing	DRC material temperature

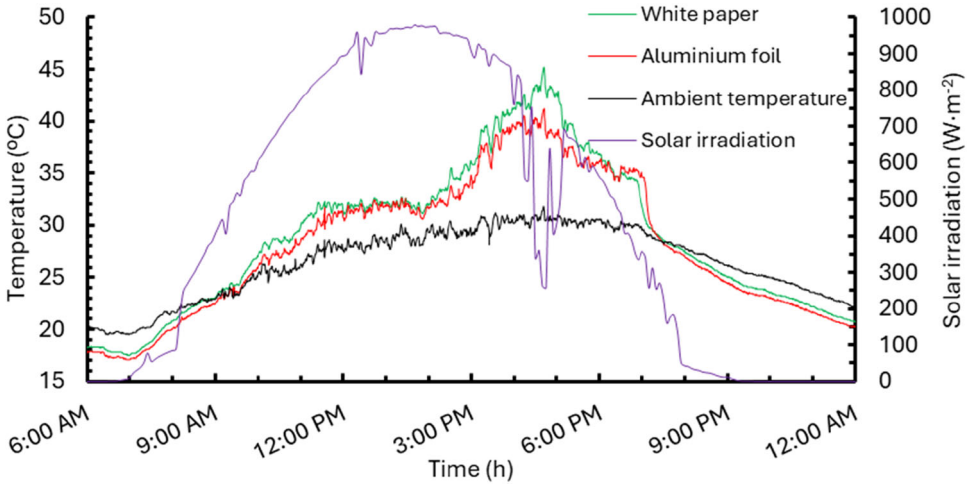

FIGURE 10 | Temperature evolution of the lateral walls with white paper and aluminum foil. [Color figure can be viewed at wileyonlinelibrary.com]

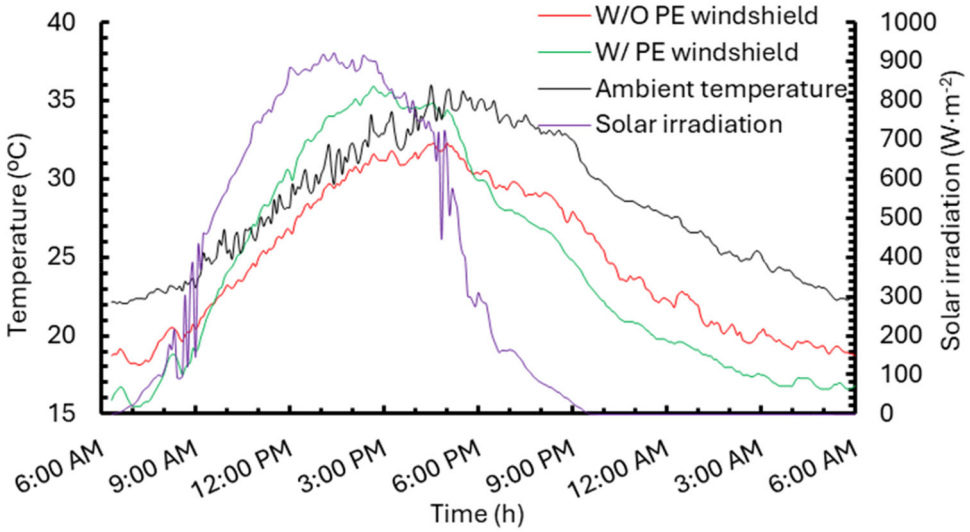

FIGURE 11 | Temperature evolution of the DRC material samples for both test boxes with and without windshield. [Color figure can be viewed at wileyonlinelibrary.com]

and 3:00 p.m. A maximum difference of 5°C is shown around 5:00 p.m.

6.2 | Impact of the Windshield Cover

In this section, the impact of the presence of a windshield cover on the test box is examined by considering two options: LDPE film of 60-μm thick and no windshield.

Figure 11 shows the temperature evolution of the samples in both test boxes, with and without 60 μm LDPE windshields for 24 h. It can be seen clearly that the windshield significantly impacts the sample temperature. The sample temperature in the test box with the LDPE cover is greater than the sample temperature in the test box without the LDPE cover during the higher solar irradiation period. During the day, the sample in the test box without the LDPE windshield remains below the ambient temperature, and a maximum sub-ambient temperature of 5.8°C is achieved. This is because the LDPE cover creates the greenhouse effect in the enclosed air gap, and temperatures above the ambient temperatures are achieved from 11:30 a.m. to 5 p.m. At night, the two samples' temperatures are below the ambient temperature, but the sample in the test box with the windshield achieves lower temperatures compared to the sample in the test box with no windshield cover. This is the expected effect of the windshield, increasing the thermal resistance from the ambient air to the DRC sample and so allowing a higher sub-ambient cooling. The maximum sub-ambient temperatures achieved during the night are 8.2°C and 5.6°C for samples in the test box, with and without PE windshield, respectively.

The temperature of the enclosed air of the test boxes with and without windshield is also presented in Figure 12. It can be noticed that the temperature of the enclosed air in both test boxes is higher than the ambient temperature, with the test box using an LDPE windshield exhibiting significantly higher air temperatures during the daytime period. This increase is primarily due to the greenhouse effect, as LDPE is not fully

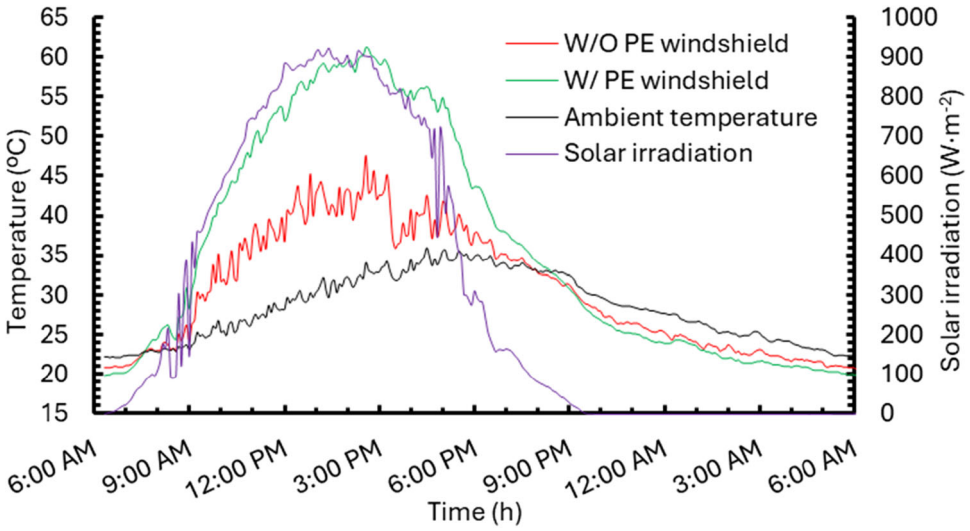

FIGURE 12 | Temperature evolution of the enclosed air for both test boxes with and without windshield. [Color figure can be viewed at wileyonlinelibrary.com]

transparent in the infrared spectrum, with a transmissivity of approximately 84%. Consequently, while LDPE allows a portion of the incident solar radiation to pass through, it partially absorbs and re-emits longwave infrared radiation, leading to heat accumulation inside the enclosed air volume. From an energy balance perspective, the enclosed air in the test box with the LDPE windshield experiences a reduction in radiative heat loss to the sky due to the windshield's infrared opacity. The absorbed infrared radiation is re-emitted within the enclosure, increasing the air temperature. This trapped longwave radiation effectively prevents the sample from fully dissipating heat, contributing to the overall warming effect. On the other hand, in the test box without a windshield, there is no enclosed air volume, allowing for natural convective mixing with the ambient air. This promotes better heat dissipation, although the temperature of the test box air remains higher than ambient during the daytime due to direct solar heating. The absence of an infrared-opaque barrier enables more effective longwave RC to the sky, contrasting with the behavior observed in the windshield-covered test box. It can also be seen that the temperature of the test box air in the case of no windshield is higher than the ambient temperature during daytime. This is because the ambient temperature is measured using the Stevenson windshield while the RTD sensors of the test box are shaded using a cardboard shade, and the shader itself is heated up due to solar radiation. For this, the impact of the shader of the RTD sensor is investigated in the following sub-section.

During the night, the air in both test boxes is lower than the ambient temperature. Lower temperatures are observed with the presence of a windshield. When using windshields in nighttime RC, the enclosed air temperature is 1°C below the temperature of the test box without windshield during most of the night.

6.3 | Impact of the Shader Material Used for the Ambient Temperature Sensor in the Test Box

A shader is used in the test box to prevent the enclosed air temperature sensors from overheating due to direct solar radiation. Thermal imaging demonstrated that the shader itself was a hot spot (Figure 13 [left]), presenting an estimated temperature of 56.2°C compared to the 39.7°C estimated for the background covered by the white paper. This is because the cardboard material initially selected as the shader has high solar absorptivity and contributes to heat collection at that zone.

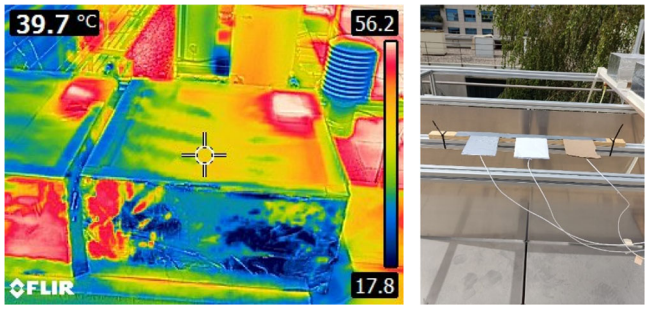

FIGURE 13 | Thermographic imaging of the test box (left) and shader materials (right). [Color figure can be viewed at wileyonlinelibrary.com]

To prevent the shader from overheating and consequently prevent the enclosed air temperature sensors from gaining this extra heat, three different shaders with the same dimensions of 7×11 cm are considered and tested on a high solar radiation day: one covered with white paper, another covered by aluminum foil and a third one not modified at all (bare cardboard), as shown in the Figure 13 (right).

It is observed that the temperature of the three shaders has the same evolution with time (Figure 14). From 12:00 p.m to 6:00 p.m, the three shaders reach the peak temperature. The maximum shader temperatures recorded during this test are 43.8°C, 41.2°C, and 39°C for bare cardboard, shader covered by aluminum foil, and shader covered by white paper, respectively. It is noticeable that the cardboard shader covered by white paper has a lower temperature under the effect of solar radiation compared to the other shaders, and the bare cardboard shader is the worst choice as a shader because of its higher

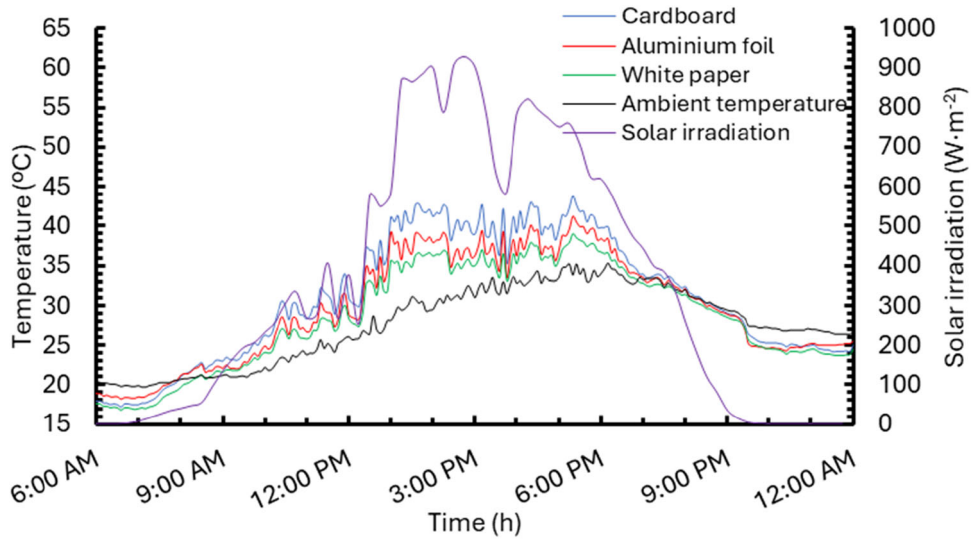

FIGURE 14 | Temperature evolution of the three types of shaders. [Color figure can be viewed at wileyonlinelibrary.com]

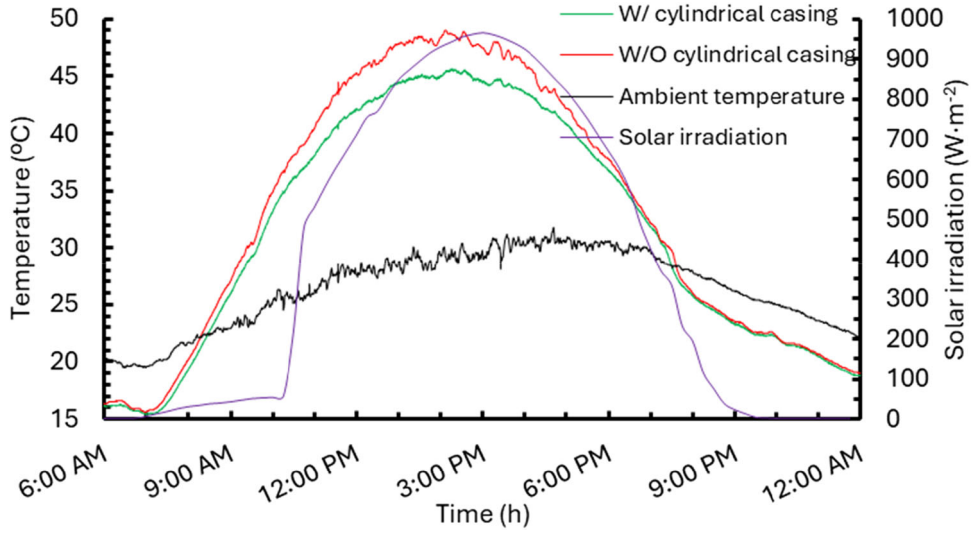

FIGURE 15 | Temperature evolution of the enclosed air with and without cylindrical casing. [Color figure can be viewed at wileyonlinelibrary.com]

temperature since it absorbs solar heat under the effect of solar radiation.

6.4 | Impact of the Cylindrical Casing in the Enclosed Air Temperature

Figure 15 shows the temperature evolution of the enclosed air in the two test boxes for one day. In both test boxes, the temperature of the enclosed air increases during the day because of the increasing solar radiation. The peak temperatures of the enclosed air with and without cylindrical casing are 45.7°C and 49°C, respectively. The maximum temperature difference between the two test boxes is 3.3°C.

6.5 | A Case Study of Daytime RC Material

A case study of the substrate material of the sample and the DRC material (CHILLSKYN) is investigated to show its impact on the RC behavior. For this investigation, the results of the previous section are used to construct a test box to test daytime RC materials. The test box designed is a wooden box with lateral walls covered by aluminum foil. A white paper is used to cover the background surface facing the sky, and the enclosed air temperature sensor is protected by a white paper-covered cardboard shader and the cylindrical casing. Finally, the 60 μm LDPE is used as a windshield for the test box [21, 22]. Figure 16 presents an image of the final test box.

The temperature evolution of the sample and the enclosed air as a function of time and climatic conditions is shown in Figure 17. The sky was clear at midday and partially cloudy at the start and at the end of the day. The solar irradiation has a peak of 676 $W \cdot m^{-2}$ at 1:31 p.m. The relative humidity was higher at night and reached 90%, and it had lower values during the day, with a mean value of about 48%.

During the night, the temperature of the sample is below ambient temperature. A sub-ambient temperature of about 10°C

is obtained. Also, the enclosed air temperature shows sub-ambient temperatures of about 3.5°C.

During the day, as solar irradiation increases, the temperature of the sample also increases. It is observed that the temperature of the sample of copper substrate is always under ambient temperature, even at the peak values of the solar irradiation, with a sub-ambient temperature of 0.3°C. As the solar irradiation increases, the temperature of the enclosed air also increases and surpasses the ambient temperature, with a peak value of 40°C, about 13°C above the sample temperature. Thus, obviously, this overheated air trapped is affecting the energy balance on the surface and the final equilibrium temperature of the sample. Based on our results, the claimed benefit of the LDPE windshield, observed in many literature papers, in terms of reducing the heat transmittance between outside air and the DRC material is offset in sunny hours by the higher temperature gradient between enclosed air and sample and the consequent increase in convection heat transfer.

7 | Conclusions

The results of this study add to the current body of knowledge in the field of daytime RC by providing a useful comprehensive vision to scientists and designers who are working on creating a test box for daytime RC systems. Under the actual nocturnal and diurnal climatic conditions of Lleida, a city representative of a temperate semi-arid climate, the effects of several parameters that may influence test box thermal behavior as well as the influence of different substrate materials on the RC material temperature were examined. The impact of the test box lateral walls coating, the impact of the polyethylene windshield cover, the protection of the enclosed air temperature sensor, and the substrate material of the sample are investigated. The results of the tests lead to the following conclusions:

1. During nighttime, the use of the polyethylene windshield has a great impact. The sample temperature was, on average, 7.5°C and 4.5°C below the ambient temperature for the test box with and without PE windshield, respectively. The sample temperature difference between the test box with and without PE windshield was about 3°C.
2. During daytime RC, it is advisable to remove the polyethylene windshield since a sub-ambient temperature during all day is obtained in the case of no windshield, while a temperature of 3°C above the ambient temperature is obtained in the case of using the PE windshield because it creates an overheated air space (due to the combination of incident solar irradiation and partial greenhouse effect of the PE), which results in more convective heat transfer to the DRC sample.
3. Both aluminum and white paper are adequate materials to cover the test box surfaces and reflect solar radiation. Aluminum performs slightly better during the day, while white paper results in slightly better performances as shader and in night operation.
4. The shader and the cylindrical casing for the enclosed air temperature measurement are good options to accurately measure the temperature of the enclosed air between the sample and the PE windshield (if used) during the day since the shader prevents overheating of the sensor from direct solar radiation and the cylindrical casing prevents

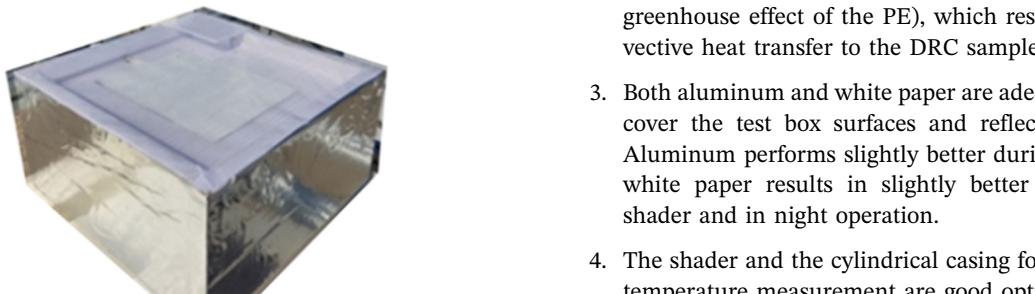

FIGURE 16 | Photography of the test box used in this study. [Color figure can be viewed at wileyonlinelibrary.com]

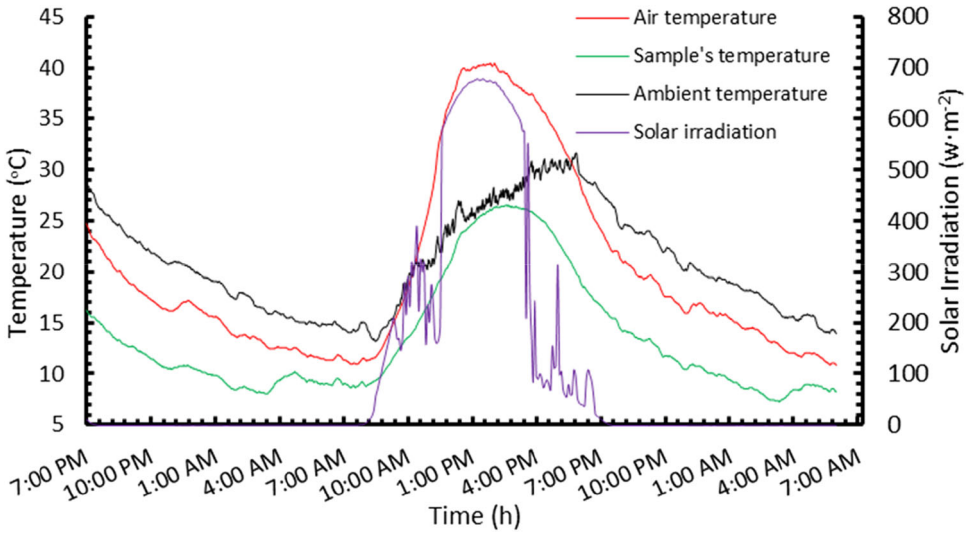

FIGURE 17 | Sample and enclosed air temperatures evolution. [Color figure can be viewed at wileyonlinelibrary.com]

from bounced solar radiation beams from the bottom to the sensor.

5. The copper substrate sample can achieve low temperatures during the day, with a maximum sub-ambient temperature of 0.3°C at the peak value of solar radiation. It was possible to achieve sub-ambient temperatures throughout the day under sunny conditions in October when the solar irradiation peak reached 676 $W \cdot m^{-2}$ for a case study with a sample consisting of copper as the substrate material and CHILLSKYN as the DRC coating.

Acknowledgments

This publication is part of the grant PID2021-126643OB-I00, funded by MCIN/AEI/10.13039/501100011033/and by "ERDF A way of making Europe". This publication is part of the grant TED2021-131446B-I00, funded by MCIN/AEI/10.13039/501100011033/and by the "European Union NextGenerationEU/PRTR". This publication is also part of the grant PDC2022-133215-I00, funded by MCIN/AEI/10.13039/501100011033/and by the "European Union NextGenerationEU/PRTR". The authors would like to thank Generalitat de Catalunya for the project awarded to their research group (2021 SGR 01370). Dr. R. Haddouche would like to thank the project INVESTIGO-AGAUR for his postdoc funding.

Data Availability Statement

The data that support the findings of this study are available from the corresponding author upon reasonable request.

References

1. B. Zhao, M. Hu, X. Ao, N. Chen, and G. Pei, "Radiative Cooling: A Review of Fundamentals, Materials, Applications, and Prospects," *Applied Energy* 236 (February 2019): 489–513, https://doi.org/10.1016/j.apenergy.2018.12.018.

2. M. Hu, G. Pei, L. Li, R. Zheng, J. Li, and J. Ji, "Theoretical and Experimental Study of Spectral Selectivity Surface for Both Solar Heating and Radiative Cooling," *International Journal of Photoenergy* 2015 (2015): 1–9, https://doi.org/10.1155/2015/807875.

3. S. Vall, M. Medrano, C. Solé, and A. Castell, "Combined Radiative Cooling and Solar Thermal Collection: Experimental Proof of Concept," *Energies* 13, no. 4 (February 2020): 893, https://doi.org/10.3390/en13040893.

4. E. Hosseinzadeh and H. Taherian, "An Experimental and Analytical Study of a Radiative Cooling System With Unglazed Flat Plate Collectors," *International Journal of Green Energy* 9, no. 8 (2012): 766–779, https://doi.org/10.1080/15435075.2011.641189.

5. E. Erell and Y. Etzion, "Heating Experiments With a Radiative Cooling System," *Building and Environment* 31, no. 6 (1996): 509–517, nov, https://doi.org/10.1016/0360-1323(96)00030-3.

6. W. Li, Y. Li, and K. W. Shah, "A Materials Perspective on Radiative Cooling Structures for Buildings," *Solar Energy* 207 (September 2020): 247–269, https://doi.org/10.1016/j.solener.2020.06.095.

7. X. Yu, J. Chan, and C. Chen, "Review of Radiative Cooling Materials: Performance Evaluation and Design Approaches," *Nano Energy* 88 (2021): 106259, https://doi.org/10.1016/j.nanoen.2021.106259.

8. J. Liu, J. Zhang, H. Tang, et al., "Recent Advances in the Development of Radiative Sky Cooling Inspired From Solar Thermal Harvesting," *Nano Energy* 81 (2021): 105611, https://doi.org/10.1016/j.nanoen.2020.105611.

9. A. P. Raman, M. A. Anoma, L. Zhu, E. Rephaeli, and S. Fan, "Passive Radiative Cooling Below Ambient Air Temperature Under Direct Sunlight," *Nature* 515, no. 7528 (November 2014): 540–544, https://doi.org/10.1038/nature13883.

10. J. Kou, Z. Jurado, Z. Chen, S. Fan, and A. J. Minnich, "Daytime Radiative Cooling Using Near-Black Infrared Emitters," *ACS Photonics* 4, no. 3 (March 2017): 626–630, https://doi.org/10.1021/acsphotonics.6b00991.

11. C. Y. Tso, K. C. Chan, and C. Y. H. Chao, "A Field Investigation of Passive Radiative Cooling Under Hong Kong's Climate," *Renewable Energy* 106 (June 2017): 52–61, https://doi.org/10.1016/j.renene.2017.01.018.

12. X. Ao, M. Hu, B. Zhao, N. Chen, G. Pei, and C. Zou, "Preliminary Experimental Study of a Specular and a Diffuse Surface for Daytime Radiative Cooling," *Solar Energy Materials and Solar Cells* 191 (March 2019): 290–296, https://doi.org/10.1016/j.solmat.2018.11.032.

13. N. Li, J. Wang, D. Liu, et al., "Selective Spectral Optical Properties and Structure of Aluminum Phosphate for Daytime Passive Radiative Cooling Application," *Solar Energy Materials and Solar Cells* 194 (June 2019): 103–110, https://doi.org/10.1016/j.solmat.2019.01.036.

14. J. Liu, Z. Zhou, D. Zhang, et al., "Field Investigation and Performance Evaluation of Sub-Ambient Radiative Cooling in Low Latitude Seaside," *Renewable Energy* 155 (2020): 90–99, https://doi.org/10.1016/j.renene.2020.03.136.

15. D. Han, B. F. Ng, and M. P. Wan, "Preliminary Study of Passive Radiative Cooling Under Singapore's Tropical Climate," *Solar Energy Materials and Solar Cells* 206 (2020): 110270, https://doi.org/10.1016/j.solmat.2019.110270.

16. J. Liu, J. Zhang, D. Zhang, et al., "Sub-Ambient Radiative Cooling With Wind Cover," *Renewable and Sustainable Energy Reviews* 130 (2020): 109935, https://doi.org/10.1016/j.rser.2020.109935.

17. R. Y. M. Wong, C. Y. Tso, S. Y. Jeong, S. C. Fu, and C. Y. H. Chao, "Critical Sky Temperatures for Passive Radiative Cooling," *Renewable Energy* 211 (July 2023): 214–226, https://doi.org/10.1016/j.renene.2023.04.142.

18. Y. Zhai, Y. Ma, S. N. David, et al., "Scalable-Manufactured Randomized Glass-Polymer Hybrid Metamaterial for Daytime Radiative Cooling," *Science* 355, no. 6329 (March 2017): 1062–1066, https://doi.org/10.1126/science.aai7899.

19. Y. Zhang, X. Tan, G. Qi, et al., "Effective Radiative Cooling With ZrO_2/PDMS Reflective Coating," *Solar Energy Materials & Solar Cells* 229, (April 2021): 111129.

20. B. Xiang, R. Zhang, Y. Luo, et al., "3D Porous Polymer Film With Designed Pore Architecture and Auto-Deposited SiO_2 for Highly Efficient Passive Radiative Cooling," *Nano Energy* 81 (2021): 105600, https://doi.org/10.1016/j.nanoen.2020.105600.

21. C. Park, C. Park, S. Park, J. Lee, Y. S. Kim, and Y. Yoo, "Hybrid Emitters With Raspberry-Like Hollow SiO_2 Spheres for Passive Daytime Radiative Cooling," *Chemical Engineering Journal* 459 (2023): 141652, https://doi.org/10.1016/j.cej.2023.141652.

22. S. Liu, F. Zhang, X. Chen, H. Yan, W. Chen, and M. Chen, "Thin Paints for Durable and Scalable Radiative Cooling," *Journal of Energy Chemistry* 90 (March 2024): 176–182, https://doi.org/10.1016/j.jechem.2023.11.016.

23. J. Lee, D. Im, S. Sung, et al., "Scalable and Efficient Radiative Cooling Coatings Using Uniform-Hollow Silica Spheres," *Applied Thermal Engineering* 254 (2024): 123810, https://doi.org/10.1016/j.applthermaleng.2024.123810.

24. J. Yu, C. Park, B. Kim, et al., "Enhancing Passive Radiative Cooling Films With Hollow Yttrium-Oxide Spheres Insights From FDTD Simulation," *Macromolecular Rapid Communications* 46, no. 3 (2025): 2400770, https://doi.org/10.1002/marc.202400770.

25. PDRC | CHILLSKYN Solutions, "ChillSkyn - PDRC," https://www.chillskyn.com.

26. M. R. Haddouche, J. Ferreira, B. D. Mselle, et al., "Design Strategies for Testing Daytime and Night-Time Radiative Cooling," in *Proceeding*

of the 13th National and 4th International Conference in Engineering Thermodynamics, (December 202).

27. M. R. Haddouche, J. Cofre-Toledo, C. Sole, et al., "Numerical Investigation of a Test Box for Radiative Cooling Materials," *Avances en Ciencias y Técnicas del Frío - 12. Actas del XII Congreso Ibérico y X Congreso Iberoamericano de Ciencias y Técnicas del Frío CYTEF* (2024): 79, https://doi.org/10.21134/xs0ghs82.

28. See, https://ennologic.com/wp-content/uploads/2018/07/Ultimate-Emissivity-Table.pdf.